Structural and Kinetic Properties of α-Tocopherol in Phospholipid Bilayers, a Molecular Dynamics Simulation Study

Shan-Shan Qin and Zhi-Wu Yu*

Key Lab of Bioorganic Phosphorous Chemistry & Chemical Biology (Ministry of Education), Department of Chemistry, Tsinghua University, Beijing 100084, P. R. China

Yang-Xin Yu

Department of Chemical Engineering, Tsinghua University, Beijing 100084, P. R. China

Received: August 2, 2009; Revised Manuscript Received: October 27, 2009

Structural and kinetic properties of vitamin E in biomembranes provide the key to understanding the biological functions of this lipophilic vitamin. We report a series of molecular dynamics simulations of two α-tocopherol/phosphatidylcholine systems and two α-tocopherol/phosphatidylethanolamine systems in water at 280, 310, and 350 K. The preferential position, hydrogen bonding, orientation, and dynamic properties of the α-tocopherol molecule in the bilayers have been examined. In all the four systems simulated, the vitamin remains in one leaflet of lipid bilayer at 280 and 310 K but flips over from one side to the other at 350 K within 200 ns of the simulation. The hydroxyl oxygen in the headgroup of α-tocopherol preferred a location between the third and the fifth carbon atom in the *sn*-2 acyl chains of the lipids. Hydrogen bonding analysis shows that the hydrogen bonds are mainly with the oxygens of the fatty acid esters rather than with the phosphate oxygens of the lipid molecule, and those with the amino groups are trivial in the case of phosphatidylethanolamines, at all three temperatures. The hydrogen bonds with phosphatidylethanolamines are more stable than those with phosphatidylcholines at low temperatures. The orientation of α-tocopherol in the bilayers is relatively flexible: the chromanol ring takes various tilt angles with respect to the bilayer normal, and the isoprenyl chain is mobile and able to adopt many different conformers. Calculation of lateral diffusion coefficients of α-tocopherol and phospholipid molecules shows that α-tocopherol has a comparable diffusion rate with phospholipid molecules at the gel phase but diffuses more rapidly than lipid molecules at the liquid-crystal phase.

1. Introduction

A vitamin deficiency in rats was first described by Evans and Scott Bishop[1] working in 1922 at the University of California, Berkeley, which they designated factor X. The fat-soluble vitamin, known as vitamin E, was subsequently characterized by Fernholz in 1938.[2] Vitamin E includes all tocol and tocotrienol derivatives with biological activity.[3] The most abundant form is α-tocopherol (Figure 1), which accumulates preferentially in mammalian tissues although it is not necessarily the most abundant form in the diet. This is due to specific retention of the *RRR*-α-tocopherol stereoisomer by tocopherol-binding proteins.[4,5]

α-Tocopherol is believed to have primarily two functions: to protect the tissues especially those containing unsaturated lipids from free radical damage[3,7] and to stabilize the structure of membranes by forming complexes with destabilizing molecules.[6,7] The fat-soluble vitamin is sparingly soluble in water and locates preferentially in cell membranes and lipoproteins.[7] The putative role of tocopherol as membrane antioxidants and stabilizers depends on their orientation and location in cell membranes. The manner in which they are arranged and distributed within membranes is presumed to govern the molecular mechanisms underlying these functions. There have been numerous experimental studies of phospholipid model membranes which aim to explain how vitamin E interacts with biological membranes. Quinn investigated the α-tocopherol/dipalmitoylphosphatidylcholine (DPPC) system in 1995[8] and found that the presence of α-tocopherol apparently eliminated the pretransition enthalpy, and the mixture exhibited phase separation of pure phospholipid from an α-tocopherol-enriched domain in both gel and liquid-crystal states. Wang et al.[9] studied the mixed aqueous dispersions of saturated phosphatidylcholines (PCs) and α-tocopherol using X-ray diffraction and freeze-fracture electron microscopic methods and pointed out that a ripple phase was observed in all of the mixtures at temperatures well below the pretransition temperature of the corresponding pure phospholipids. These workers also reported that α-tocopherol induces nonlamellar phases in aqueous dispersions of dipalmitoylphosphatidylethanolamine (DPPE).[10] Disturbance of the packing of the acyl chains by the presence of α-tocopherol was reported from ESR[11] and NMR[12] spectroscopic studies. Steady state[13] and time-resolved[14] fluorescence anisotropy measurements of probes interpolated into phospholipid dispersions or membranes indicated that α-tocopherol causes an increase in order parameter and decrease in fluidity of the hydrocarbon domain of the structures at the liquid-crystal phase. As for computational study on α-tocopherol/lipid complexes, Shamovski and Yrovskaya searched the potential energy global minimum of molecular complexes of α-tocopherol with 1-stearoyl-2-arachidonyl-phosphatidylcholine and 1-stearoyl-2-

* To whom correspondence should be addressed. E-mail: yuzhw@tsinghua.edu.cn.

10.1021/jp9074306
Published on Web 11/23/2009

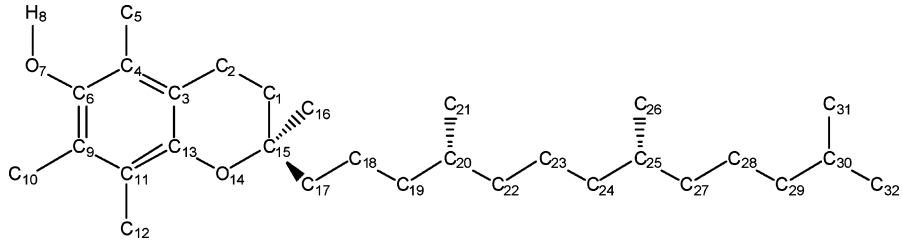

Figure 1. Molecular structure of α-tocopherol with the assigned atom numbers.

arachidonyl-phosphatidylethanolamine using Monte Carlo and MMP2 techniques.[15]

The precise location and orientation of α-tocopherol in membrane lipid bilayers are still subject to conjecture. Spectroscopic studies by Srecastava et. al[16] indicated that α-tocopherol interpolates into bilayers of DPPC with the chromanol ring situated at the aqueous interface of the structure. Fluorescence quenching based on paramagnetic resonance and ^{13}C magnetic resonance studies of α-tocopherol in bilayers of DPPC[17] indicated a location of the chromanol ring of α-tocopherol about 1 nm from the aqueous interface. Quenching of tocopherol fluorescence by the anthroyloxy group located at specific positions of stearic acid showed an order of tocopherol fluorescence quenching efficiency 7-AS > 2-AS > 9-AS = 12-AS, suggesting that the chromanol fluorophore resided between the 2- and 7-position of the stearic acid chain but closer to the latter in PC bilayers of different degrees of unsaturation.[18,19] In another fluorescence quenching experiment using DOXYL stearates, it was found that the average location of tocopherol in dilinoleoyl−PC bilayers was between two extremities:[20] the chromanol ring is slightly recessed back into the membrane, and its hydroxyl group may be hydrogen bonded to either phosphate oxygen or acyl-ester oxygen atoms; or the chromanol is deeply submerged into the bilayer, closer to the conjugated double bonds.

In addition to the location and orientation of the α-tocopherol inside the membrane, the mobility of α-tocopherol scaled by a diffusion constant is also rarely investigated experimentally. Gramlich et al.[21] studied the quenching of α-tocopherol by time-resolved fluorescence in the environment of 1-palmitoyl-2-oleoyl-phosphatidylcholine (POPC) liposomes and found that the lateral diffusion coefficient for α-tocopherol is 1.8 (±0.1) $\times 10^{-7}$ cm^2 s^{-1}, about a factor of 2 larger than that of POPC itself.

Since the molecular details of α-tocopherol in biomembranes is uncertain, we have undertaken a computational investigation of a system of α-tocopherol with phospholipid bilayers. We have used standard molecular dynamics simulation methods to examine these mixtures at different temperatures out to 200 ns.

2. Computational Details

2.1. Simulation Conditions. The simulation included one α-tocopherol molecule in the upper leaflet, 63 phospholipid molecules (31 in the upper layer and 32 in the lower), and more than 43 water molecules per lipid molecule to attenuate the influence of the image bilayer. The proportion of α-tocopherol in the ensemble was in the same order as found in Golgi membranes and lysosomes, where the molar ratio is in the order of 1:65.[22,23] Periodic boundary conditions in X, Y, and Z directions were used. Simulations of the binary α-tocopherol/phospholipid systems have been carried out at 280, 310, and 350 K, at which model membranes would be in either gel or liquid-crystal state. Four representative phospholipids were selected in our study: two saturated lipids dipalmitoylphosphatidylcholine (DPPC) and dipalmitoylphosphatidylethanolamine (DPPE), and two unsaturated lipids 1-palmitoyl-2-oleoyl-phosphatidylcholine (POPC) and 1-palmitoyl-2-oleoyl-phosphatidylethanolamine (POPE). All the simulations started with the configuration with α-tocopherol vertically inserted into the middle of the phospholipid bilayer in the upper leaflet with the chromanol ring close to the lipid−water interface or the glycerol backbone. The simulation time for each system was 200 ns, and only the trajectory for the last 40 ns was used for analysis. We also performed simulations with the different configuration that α-tocopherol initially stayed in the center of the lipid bilayers. It was found that the molecule moved to one of the leaflets with its head orienting toward the lipid−water interface after about tens of nanoseconds of simulation. Thus, only the results for the first configuration were analyzed.

All the simulations were carried out in the NPT ensemble, at constant pressure of 1 bar and various temperatures. The time step was 2 fs for all simulations, and the pair list for computing nonbonded pair forces was updated every 10 steps with a list-cutoff of 0.9 nm. The coulomb and van der Waals interactions were computed using the cutoff algorithm, and the cutoff radius for both coulomb and van der Waals interactions was 0.9 nm. The long-range electrostatic interaction was corrected using the PME method,[24,25] with the maximum spacing for the FFT grid of 0.12 nm and the interpolation order of 4. The weak coupling scheme of Berendsen and co-workers[26,27] was used for both temperature and pressure control, with the temperature coupling time constant of 0.1 ps. For pressure coupling, we used the semiisotropic coupling type, with the coupling time constant of 1.0 ps and the compressibility of 4.6×10^{-5} bar^{-1}. The trajectory was collected every 2 ps, and all the simulations were performed with the Gromacs 3.3.1 package[28,29] in parallel under a Windows Compute Cluster Server.

2.2. Molecular Models. For lipid models, the bonded parameters were from Peter Tieleman's Web site,[30] and the Ryckaert−Bellemans potential[31] was used as the torsion potential of the lipid hydrocarbon chains. For nonbonded parameters, we used values from Berger et al.[32] for lipid tails and OPLS values[33,34] for headgroups, and the partial atomic charges were obtained from Chiu et al.[35] For water molecules, the SPC model[36] was used with settle algorithm[37] to constrain bonds and angles. All the CH3, CH2, and CH groups were treated as united atoms, and hydrogen atoms in the amino group of phosphatidylethanolamines were considered explicitly due to their capability to form hydrogen bonds.

For α-tocopherol, we proposed a united atom model, and the hydrogen atom in the hydroxyl group was described explicitly to keep the accurate hydrogen bonding properties of the hydroxyl group. The Lennard-Jones parameters were from the original OPLS Lennard-Jones parameter set.[33,34] This has been done to adjust the nonbonded interaction to the OPLS Lennard-Jones parameters of the phospholipid model. The harmonic potentials describing bonds, angles, and dihedral angles were taken from the Amber 2003 united atom force field.[38,39] We

have carefully evaluated the energetical profile of the tocopherol tail by calculating the torsional barriers in three isopentyl fragments at the HF/6-31G* level using Gaussian98[40] and the MD model by vacuum simulations of the same isopentyl fragments. This comparison gave a good agreement between MD simulations and quantum chemical calculations. The charges in the molecule are determined by the two-stage resp method[41] from an HF/6-31G* optimized α-tocopherol geometry.

The lipid force field adopted in this work was originally developed for simulating lipid bilayers at the liquid-crystal state. The model has been shown to yield an excellent agreement with experiments with respect to the lipid area, volume and density, orientational order parameters of the hydrocarbon chains, and distances of certain carbon pairs in the palmitic tails at the liquid-crystal phase.[32] To test the validity of the force field of α-tocopherol, we calculated the density of α-tocopherol at room temperature and the crystal structure of the complex formed between *Vipera russelli* phospholipase A2 and α-tocopherol. For density simulation, we used an NPT ensemble at a constant pressure of 1 bar and constant temperature of 300 K. The simulation included 50 α-tocopherol molecules and lasted for 40 ns (the last 20 ns was used for analysis). The density we obtained based on our force field of α-tocopherol model was 948 kg/m^3 which was very close to the experimental value of 950 kg/m^3 at the temperature.[42] For the simulation of crystal structure, we performed an NVT simulation with the starting structure measured by X-ray diffraction[43] (pdb code 1KPM), and simulation parameters were set at 100 K, according to the conditions under which the diffraction data were collected. We adopted the OPLSAA force field[44−49] for describing *Vipera russelli* phospholipase A2, and the simulation time was 10 ns. The time-averaged root mean fluctuation of atomic positions in α-tocopherol and *Vipera russelli* phospholipase A2 over the last 8 ns after fitting to the experimental crystal structure was calculated. The results were 0.13 and 0.17 A, respectively. We thus concluded that the force field could retain the crystal structure of the complex formed between *Vipera russelli* phospholipase A2 and α-tocopherol.

As discussed above, both the lipid and the α-tocopherol models have been carefully evaluated. For the lipid−α-tocopherol system, there are only a few experimental properties that can be used to validate the reliability of the mixed lipid model. Suzuki et al.[11] examined α-tocopherol for its effect on the molecular order of phospholipids using a conventional ESR spin-label method and found that α-tocopherol disordered the gel phase and stabilized the liquid-crystalline phase. To find out whether our simulation can give comparable results, the order parameter S_{CD} of the acyl tails of phospholipid in four α-tocopherol/lipid systems has been calculated, and the results are included in the Supporting Information. For the α-tocopherol/DPPC system, the S_{CD} values for carbon atoms in the *sn*-2 acyl chain give plateau values of 0.178, 0.156, and 0.134 at 280, 310, and 350 K, respectively. In the absence of α-tocopherol, the values are 0.187, 0.150, and 0.131 at the respective temperatures. According to previous simulation work,[50] the DPPC bilayer would be in the gel phase at 280 K and the liquid-crystal phase at 310 and 350 K based on the lipid model we adopted, despite that the real transition temperature is 315 K. This means that our model correctly predicted the destabilizing effect of α-tocopherol on the gel phase and the stabilizing effect on the liquid-crystal phase of DPPC. The same conclusions can be drawn for the other three lipids.

3. Results and Discussion

Molecular dynamics simulations have been performed to study both the structural and kinetic properties of α-tocopherol situated in four phospholipid bilayers at various temperatures. To get a general view of how α-tocopherol locates in various lipid bilayers, selected snapshots of the α-tocopherol/DPPC system at 280, 310, and 350 K are shown in Figure 2 as representative pictures. At 280 and 310 K, α-tocopherol stays in the initial upper leaflet of the DPPC bilayer during the simulation time as judged by the location of the hydroxyl group, while at 350 K, α-tocopherol appears on both the upper and lower leaflets of the bilayer, indicating the "flip-flop" moving mode of the molecule at high temperatures in the lipid bilayer. Such a "flip-flop" phenomenon of tocopherol has also been observed in three other lipid bilayers at 350 K. Generally speaking, the α-tocopherol molecule, or separately its head and tail, can take many different conformations in the examined four lipid bilayers. Detailed statistical analysis of the simulation results will be discussed in the following sections.

3.1. Position of α-Tocopherol in Lipid Bilayers. *α-Tocopherol/DPPC System.* To describe the relative location of α-tocopherol in the DPPC bilayer quantitatively, we calculated the number density $\rho(Z)$ of atom O7 in the headgroup and atom C32 in the tail chain of α-tocopherol, along the membrane normal at 280, 310, and 350 K, respectively. We also calculated the number density of phosphorus atoms in the lipid headgroups at these temperatures for comparison. The center of the lipid bilayer is used as the origin. The results are shown in Figure 3. At 280 K, the peak value of the number density of atom O7 in α-tocopherol locates at 1.33 nm, and that of phosphorus atoms in DPPC locates at 1.83 nm (Figure 3a1). The difference is 0.50 nm. These data show that the headgroup of α-tocopherol lies in the middle part of the upper leaflet but closer to the membrane interface in comparison with that of the tail end. This is due to the hydrophilic property of the hydroxyl group in the headgroup of α-tocopherol. The isoprenoid tail of α-tocopherol has a wider density distribution overlapping with its headgroup, representing a larger moving range.

At 310 K, the peak value of the number density of atom O7 in α-tocopherol locates at 1.14 nm, and that of phosphorus atoms in DPPC headgroups locates at 1.88 nm to the bilayer center (Figure 3a2). The bigger difference of 0.74 nm means that the headgroup of α-tocopherol stays a little bit away from DPPC headgroups in comparison with the situation at 280 K.

Most interestingly, two maxima of the number density of atom O7 are seen on both sides of the origin in the $\rho(Z)$ curve at 350 K (Figure 3a3), indicating that the headgroup of α-tocopherol appears in both the upper and lower leaflets of the DPPC bilayer, representing a "flip-flop" moving mode. This is explained as that at such high temperature the α-tocopherol molecule has high enough energy to break the hydrogen bond between the hydroxyl group of α-tocopherol and the oxygen of the DPPC headgroup, allowing its headgroup to overcome the energy barrier for escaping from the hydrophilic environment and getting through the hydrophobic interior of the lipid bilayer. The isoprenoid tail of α-tocopherol stays in the middle range of the DPPC bilayer due to its hydrophobic character. Snapshots in Figure 2 show evidently a flip-flop process happening from 163.21 to 163.82 ns at the temperature.

α-Tocopherol/POPC System. Figure 3b shows the results of the α-tocopherol/POPC system. These graphs are not very different from those of the α-tocopherol/DPPC system. α-Tocopherol stays in the upper leaflet of the POPC bilayer at 280 and 310 K and flips over between the two leaflets at 350 K. At

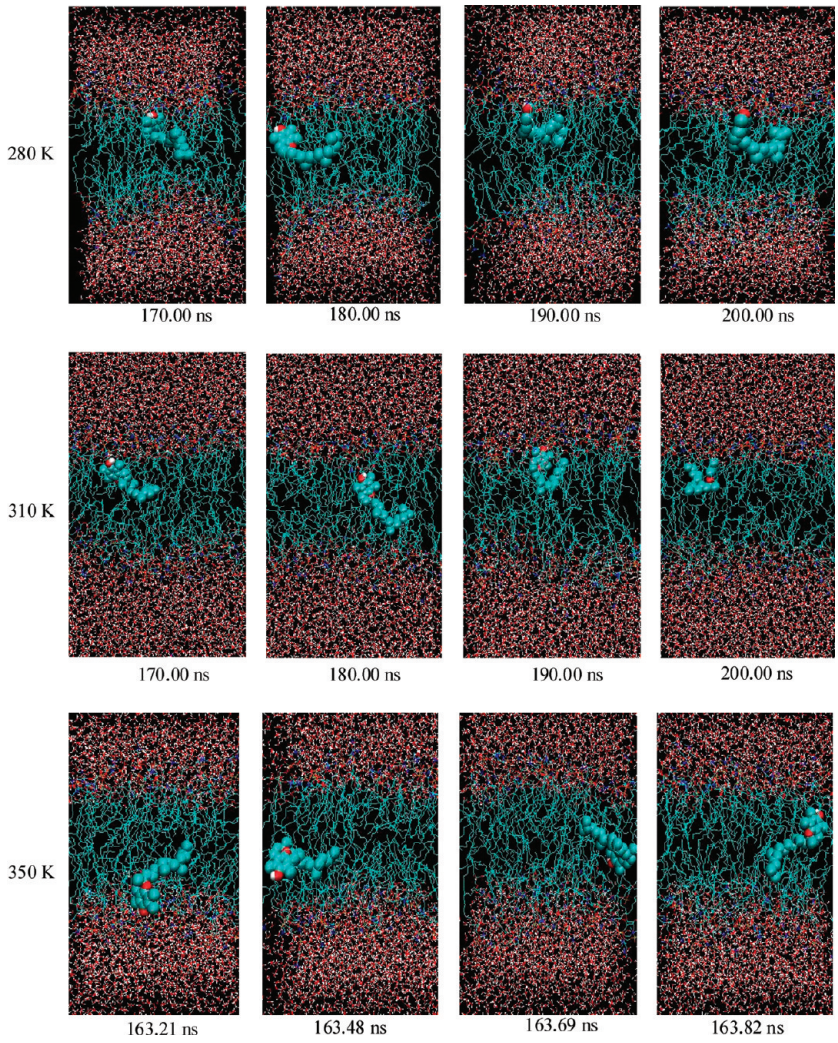

Figure 2. Snapshots of α-tocopherol/DPPC configurations at three temperatures.

280 K, the peak value of the number density of atom O7 in the α-tocopherol headgroup locates at 1.38 nm, and that of phosphorus atoms in POPC headgroups locates at 1.84 nm; at 310 K, the two values become 1.13 and 1.83 nm, implying that the headgroup of α-tocopherol stays further away from the POPC headgroup at 310 than at 280 K.

α-Tocopherol/DPPE System. Results of the α-tocopherol/DPPE system are shown in Figure 3c. It can be seen that at 280 and 310 K α-tocopherol keeps lying in one leaflet of the DPPE bilayer and flips over between the two leaflets at 350 K. The distances between the peak locations of the density profiles of atom O7 in α-tocopherol and those of the phosphorus atoms in DPPE are 0.75 and 0.80 nm at 280 and 310 K, respectively. The head of α-tocopherol moves a little farther away from the DPPE headgroup when temperature increases, which is similar to the two phosphotidylcholine systems discussed above.

α-Tocopherol/POPE System. Figure 3d shows the results of the α-tocopherol/POPE system. Like in the DPPE bilayer, α-tocopherol keeps lying in one leaflet of the POPE bilayer and flips over between the two leaflets at 350 K. The distances between the peak locations of the density profiles of atom O7 in α-tocopherol and those of the phosphorus atoms in POPE are 0.58 and 0.72 nm at 280 and 310 K, respectively, indicating that the headgroup of α-tocopherol moves away from the headgroup of the POPE bilayer when temperature increases from 280 to 310 K like the situation in the other three systems.

We can find that in all four α-tocopherol/lipid systems flip-flop takes place at 350 K but not at 280 and 310 K. Clearly, a higher temperature provides higher kinetic energy to the α-tocopherol molecule, but the four lipid species are not the same. According to the calculated coordinates of atom O7 at 350 K in four systems, α-tocopherol flips faster in POPC and POPE than in DPPC and DPPE bilayers. This can be explained as a result of the higher fluidity of the former two phospholipids due to the presence of an unsaturated bond in the s*n*-2 acyl chain of the lipid molecules.

Average Atom Positions. To get more accurate information about the relative position of the hydroxyl group of α-tocopherol in the four lipid bilayers, we calculated the average *Z*-axis value of atom O7 in α-tocopherol and the C1′−C10′ carbon atoms in the lipid *sn*-2 acyl chain numbered from C═O to the tail end at 280 and 310 K. Absolute values of distances from the bilayer center are calculated at 350 K. The results are listed in Table 1. Two main conclusions can be drawn from the table. First, the hydroxyl group locates preferably between C3′ and C5′ in all four lipid bilayers at 280 and 310 K. Particularly, at the latter temperature, the average O7 positions are all at or around C5′. This shows clearly that the hydrophilic group of α-tocopherol prefers to stay at a position below the polar region of the lipid monolayer. This is explained as that the hydrophilic character of α-tocopherol is much weaker than its hydrophobic character, and this conclusion is consistent with previous experimental

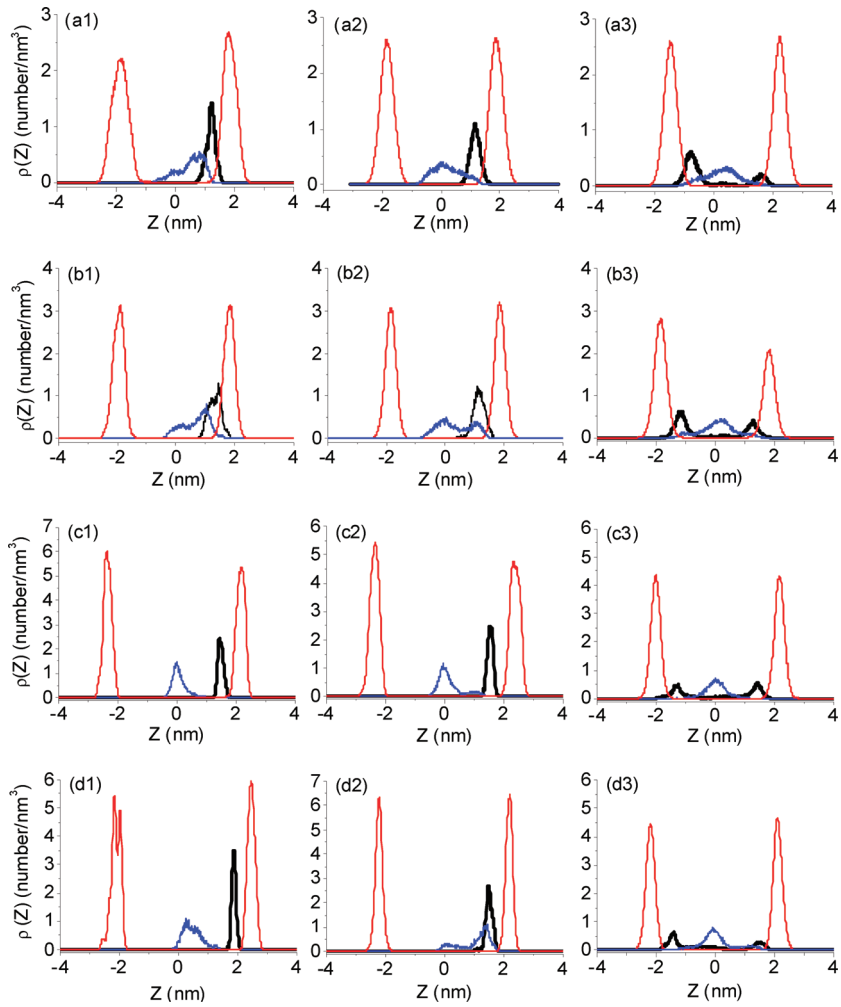

Figure 3. Number density $\rho(Z)$ of atom O7 (black) and C32 (blue) in the α-tocopherol molecule and phosphorus atoms (red) in lipid molecules along the membrane normal in four α-tocopherol/phospholipid systems. a, b, c, and d represent DPPC, POPC, DPPE, and POPE systems, and 1, 2, and 3 represent 280, 310, and 350 K, respectively. The number density of α-tocopherol is multiplied by a factor of 10 for clarity.

TABLE 1: Averaged *Z*-Axis Values (nm) of O7 in α-Tocopherol and that of C1′−C10′ in the Lipid *sn*-2 Tail at 280 and 310 K[a]

atom[b]	DPPC			DPPE			POPC			POPE		
temp/K	280	310	350	280	310	350	280	310	350	280	310	350
O7	1.49	1.27	1.14	1.53	1.38	1.33	1.36	1.25	1.08	1.93	1.53	1.15
C1′	1.67	1.61	1.58	1.89	1.82	1.80	1.64	1.61	1.50	2.14	1.90	1.70
C2′	1.58	1.52	1.49	1.80	1.71	1.70	1.54	1.51	1.40	2.03	1.80	1.59
C3′	***1.49***	1.43	1.40	1.69	1.6	1.61	1.46	1.43	1.32	**1.94**	1.73	1.51
C4′	1.39	1.34	1.31	**1.59**	1.49	1.51	**1.36**	1.33	1.23	1.82	1.62	1.40
C5′	1.30	***1.25***	1.22	**1.47**	**1.37**	1.41	1.28	**1.25**	1.15	1.73	**1.53**	1.31
C6′	1.20	1.16	1.14	1.36	1.26	1.31	1.18	1.15	1.06	1.61	1.41	1.20
C7′	1.10	1.07	1.05	1.24	1.14	1.21	1.10	1.07	0.99	1.52	1.33	1.12
C8′	1.01	0.98	0.97	1.13	1.02	1.11	1.00	0.97	0.89	1.40	1.21	1.00
C9′	0.91	0.89	0.88	1.01	0.91	1.01	0.93	0.91	0.84	1.33	1.15	0.94
C10′	0.82	0.81	0.81	0.89	0.79	0.91	0.84	0.81	0.75	1.21	1.03	0.83

[a] Absolute coordinate values are calculated at 350 K. The bilayer center is taken as the origin. [b] Note: The carbon atoms in the *sn*-2 acyl chain are numbered from C═O to the tail end.

observations, where the chromanol ring was proposed to be slightly recessed back into the membrane with its hydroxyl group hydrogen bonded to either phosphate oxygen or acyl-ester oxygen atoms.[18−20]

Second, the hydroxyl group moves toward the bilayer center with increasing temperature. For α-tocopherol/DPPC and α-tocopherol/POPE systems, the average positions of O7 move from C3′ to C5′ when temperature increases from 280 to 310 K. For the α-tocopherol/POPC system, it moves from C4′ to C5′. In the case of the α-tocopherol/DPPE system, it moves from a position between C4′ and C5′ to a position very close to C5′. Such a temperature effect is simply an entropic effect. When temperature further increases to 350 K, α-tocopherol molecules are able to move closer to the bilayer center, allowing the "flip-flop" to happen. When this happens, absolute values of distances from the bilayer center are calculated. We can see from the results that α-tocopherol stays closer to bilayer centers at 350 K.

3.2. Hydrogen Bond (HB). In the last section, we found that the average *Z*-axis of O7 of α-tocopherol is below the third

TABLE 2: Percentage of Hydrogen Bonds between the Hydroxyl Group in α-Tocopherol and Oxygen and Hydrogen Atoms in Four Lipid Species

		DPPC	DPPE	POPC	POPE
		Oxygen in Lipid Headgroup (%)			
280 K	ester oxygen[a]	78 (41 + 37)	100 (100 + 0)	67 (9 + 58)	100 (0 + 100)
	phosphate oxygen	22	0	33	0
310 K	ester oxygen	94 (57 + 37)	100 (1 + 99)	97 (94 + 3)	91 (21 + 70)
	phosphate oxygen	6	0	3	9
350 K	ester oxygen	85 (56 + 29)	92 (30 + 62)	78 (53 + 25)	88 (22 + 66)
	phosphate oxygen	15	6	22	8
		Hydrogen in Phosphatidylethanolamine Headgroup (%)			
280 K	amine hydrogen		0		0
310 K	amine hydrogen		0		0
350 K	amine hydrogen		2		4

[a] Note: The two numbers in the brackets are for carbonyl and glycerol oxygen, respectively.

carbon in the *sn*-2 acyl chain. This raises a question as to whether the hydroxyl group in α-tocopherol can form hydrogen bonds with the lipid headgroups. To address this question, we calculated the percentage of hydrogen bonds formed over the last 40 ns of simulations between the hydroxyl group in α-tocopherol and the oxygen atoms in the phosphate and ester groups of lipids, as well as the hydrogen atoms in the amino groups in the case of phosphatidylethanolamines. By considering a general form of the hydrogen bond X−H···Y, the criteria of the HB formation we adopted in the work are: the X−Y distance is less than 3.5 Å, and the H−X−Y angle is less than 30°.[51,52] The results are listed in Table 2.

Several conclusions can be drawn from the table. First, the hydrogen bonds between the hydroxyl group of α-tocopherol and the amino group in the phosphatidylethanolamines can be ignored. At 280 and 310 K, the percent of hydrogen bonds in the two lipid systems is counted as zero within the simulation error. At 350 K, the percentage is merely 2 for DPPE and 4 for POPE. The results are understandable, as the amino group is on the outermost surface of a bilayer, while the hydroxyl group locates preferably below the glycerol backbone as discussed in the last section.

Second, the hydrogen bonds are mainly with the fatty acid ester groups, not with the phosphate group in a lipid molecule at all three temperatures. Because there are in total four oxygen atoms in one phosphate group and also in two ester groups, the numbers of HB in the table concerning these two types of acceptors are comparable. At 280 K, for example, the HB percentages between the hydroxyl group and the fatty acid esters are 78%, 100%, 67%, and 100% in the four lipid systems DPPC, DPPE, POPC, and POPE, respectively. But the HB percentages between the hydroxyl group and phosphate are only 22%, 0%, 22%, and 0% in the respective lipids. The general conclusion is the same at the other two temperatures. This conclusion is in agreement with the experimental observation that the hydrogen bond is with the carbonyl oxygen in DPPC bilayer at liquid-crystal phase.[53]

Third, the hydrogen bonds involving phosphatidylethanolamines are more stable than that involving phosphatidylcholines at low temperatures. This is based on the observations that the HB percentages with phosphate are 0% for DPPE at 280 and 310 K and for POPE at 280 K, and at 280 K, the HBs with the ester groups of DPPE are 100% with carbonyl oxygen and 0% with glycerol oxygen; the HBs with the ester groups of POPE are 100% with glycerol oxygen and 0% with carbonyl oxygen. The HB distributions for DPPC and POPC are much broader. The high selectivity of HB formation between α-tocopherol and phosphatidylethanolamines at low temperatures shows that the hydroxyl group of α-tocopherol stays in a position stably. This is because at these temperatures there are cross-linking hydrogen bonds between amino groups and the phosphate and ester groups in the neighboring molecules, stabilizing the headgroup regions of phosphatidylethanolamine bilayers.[54]

Fourth, increasing temperature from 310 to 350 K reduces the number of hydrogen bonds for all four lipid systems. This is due to the movement of α-tocopherol toward the bilayer center with increasing temperature as evidenced in Table 1, but this is not the case when temperature increases from 280 to 310 K for DPPC and DPPE systems. This is because the two phospholipids are saturated lipids. At 280 K, they are at the gel state, and the molecules are so tightly packed that optimal orientation of α-tocopherol in the bilayers to form more hydrogen bonds is restricted, although the average *Z*-axis of the OH group is closer to the polar region than that at 310 K.

3.3. Orientation of α-Tocopherol in Lipid Bilayers. Two vectors were defined to describe the orientation of the head and tail of the α-tocopherol molecule in a bilayer at different temperatures. For the headgroup, the vector was defined as the connection between atom C15 and O7 of α-tocopherol; for the tail, it was defined as the line from the geometry center of carbon atoms in the main chain of the α-tocopherol tail to atom C15. For each of the two vectors, there is a tilting angle between the vector and the *Z*-axis at any moment, with possible values ranging from 0 to 180°. By dividing the angle range into 180 sectors, angle distribution could be evaluated as the total number of angles that fall into each sector normalized by the overall number of angles we sampled over a time span of 40 ns.

The tilting angle distributions of both head and tail vectors of the four lipid mixtures at three temperatures are shown in Figure 4. Generally, for the head vector in each of the four systems, a single peak is seen in each of the distribution curves at 280 and 310 K, while two peaks appear at 350 K. The double-peak feature at the high temperature represents the "flip-flop" moving mode of the tocopherol molecule. Specifically, at 280 K, the distribution curves of the α-tocopherol headgroup take a maximum value at 25° in the α-tocopherol/DPPC system and 33° in the α-tocopherol/POPC system. For the tail group at the temperature, it has the peak value at 92° in the α-tocopherol/DPPC system and 68° in the α-tocopherol/POPC system. This may be due to that at 280 K the POPC bilayer is more fluid than the DPPC bilayer and has more intermolecular space, thus the α-tocopherol head is free to have a larger sloping angle in the POPC bilayer. To understand the results of the tail vectors, we examined in detail the alignment of the tail in the bilayer. It was found that for the DPPC bilayer at 280 K it is in gel state, and the tail of α-tocopherol is difficult to enter the lower

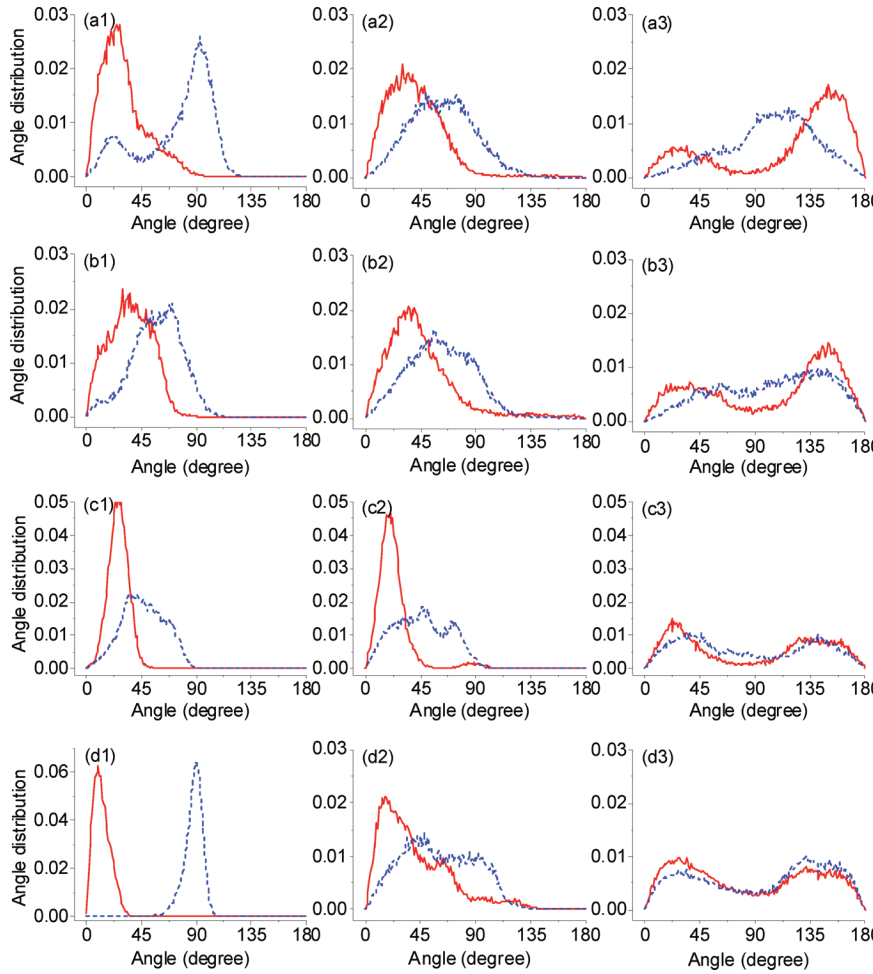

Figure 4. Normalized angle distribution of the angle between the *Z*-axis and the vectors of the head (red solid line) and tail (blue dashed line) groups of α-tocopherol in various systems at (1) 280 K; (2) 310 K; and (3) 350 K. a, b, c, and d represent DPPC, POPC, DPPE, and POPE systems, respectively.

leaflet of the DPPC bilayer; thus, it tends to lie horizontally near the bilayer center and has a tilt angle of about 90°. At 310 K, the distribution curves of the α-tocopherol headgroup take a maximum value at 30° in the α-tocopherol/DPPC system and 37° in the α-tocopherol/POPC system. For the tail group, it is 60° in the α-tocopherol/DPPC system and 58° in the α-tocopherol/POPC system. Like the situation at 280 K, the POPC bilayer has higher fluidity at 310 K, thus the headgroup of α-tocopherol is easier to be tilting in the POPC bilayer. The tail group of α-tocopherol has a comparable moving range in both lipid bilayers since the two lipid bilayers are in the liquid-crystal state,[50,55] thus it has comparable tilt angle in DPPC and POPC lipid bilayers. These results mean that the α-tocopherol head has a more sloping alignment in POPC than in the DPPC bilayer, and the tilting angle is bigger at the liquid-crystal state than at the gel state. Besides, at 310 and 350 K, the distribution curves of the α-tocopherol tail group for both systems show broader peaks than that at 280 K, indicating more random moving modes.

In α-tocopherol/phosphatidylethanolamine systems, at 280 K the distribution curves of the α-tocopherol headgroup take their maximum at 26° in the α-tocopherol/DPPE system and 10° in the α-tocopherol/POPE system, and for the tail group, it has the peak value at 40° in the α-tocopherol/DPPE system and 90° in the α-tocopherol/POPE system. To illustrate the tilt angle more intuitively, we display the snapshots of α-tocopherol/DPPE and α-tocopherol/POPE systems at 280 K in Figure 5. It can be seen from the figures that at 280 K the DPPE bilayer is tightly packed in the gel phase, and α-tocopherol is forced to be in a skew line in the DPPE bilayer. For the POPE bilayer, the lipid tail is less compact, and the α-tocopherol tail can locate horizontally in the bilayer, which leads to a much smaller tilt angle in the α-tocopherol head. At 310 K, the α-tocopherol headgroup takes its peak value at 19 and 15° in DPPE and POPE bilayers, and the tail group has a broad distribution in both α-tocopherol/DPPE and α-tocopherol/POPE systems. Since the α-tocopherol tail has a larger moving range at 310 K than that at 280 K, the tension for the α-tocopherol head becomes less in the DPPE bilayer, leading to a smaller tilt angle in the headgroup than that at 280 K. At 350 K, the α-tocopherol head has two peaks in the distribution curves in both lipid bilayers, which represents the "flip-flop" moving mode. The distribution curves of α-tocopherol are generally broader in the POPE bilayer than in the DPPE bilayer at all three temperatures, which is due to the unsaturated double bond in the POPE *sn*-2 tail that makes POPE molecules have larger area per lipid than DPPE molecules. It can be summarized from the above analysis that the α-tocopherol head has a more sloping alignment when the lipid matrix is more fluid, except for the DPPE bilayer, where the α-tocopherol tail movement is restricted by nearby DPPE molecules, which forces the α-tocopherol head to have a larger tilt angle at 280 K than that at 310 K.

3.4. Lateral Diffusion Coefficient. In addition to the structural properties of α-tocopherol in phospholipid bilayers, we

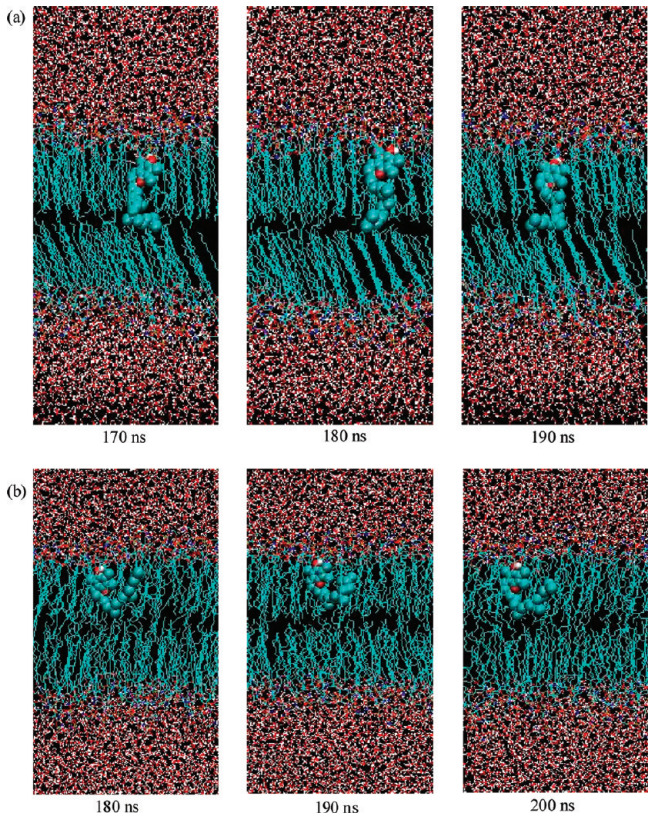

Figure 5. Snapshots of (a) α-tocopherol/DPPE and (b) α-tocopherol/POPE configurations at 280 K.

are also interested in the lateral mobility of the molecule. The diffusion coefficients can be determined from molecular dynamics simulations as the ratio of the mean square displacement (MSD) $\langle(\vec{r}(t) - \vec{r}(0))^2\rangle$ to time in the limit of infinite time

$$D = \lim_{\tau\to\infty}\left\langle \frac{|\vec{r}(t_0 + \tau) - \vec{r}(t_0)|^2}{2N_f\tau} \right\rangle$$

The brackets indicate an average over different time of the mass center of the molecules. The parameter N_f describes the number of translational degrees of freedom. For an isotropic liquid, it is three, whereas for the case of the lateral diffusion of a lipid molecule within a quasi-two-dimensional bilayer, it is two.

The lateral diffusion coefficients are obtained by calculating the average slope of the MSD plots at various intervals with a minimum of 10 ns, and the errors are estimated by calculating the standard deviation of all the slopes we obtanied. The results are listed in Table 3. There have been few experimental reports in this aspect for comparison. For pure lipid bilayers, the reported diffusion rate of DPPC is 1.1×10^{-7} cm^2 s^{-1} at 320 K,[56] and that of POPC is 1.5×10^{-7} cm^2 s^{-1} at 308 K.[57] Since quantitative comparison between experimental and calculated diffusion coefficient values is difficult due to some complications such as finite size effects[58] and our simulation with pure lipids are of the same size with mixed lipid bilayers (32 lipids in both upper and lower leaflets), the simulation results could be considered as in qualitative agreement with these experimental values. By using a novel fluorescent lipid probe and theoretical concepts that restrict tocopherol "concentrations" to a two-dimensional array, Gramlich et al.[21] assessed the diffusion coefficient of α-tocopherol in the POPC bilayer. Their calculated result was $(1.8 \pm 0.1) \times 10^{-7}$ cm^2 s^{-1} at 300 K, about a factor of 2 larger than that of POPC itself. Our simulation results are of the same order as the experimental values, thus they are qualitatively reliable to reflect the dynamic properties of α-tocopherol/lipid systems.

As can be seen in Table 3, α-tocopherol has a comparable diffusion rate with phospholipid molecules in the bilayers at the gel phase, like the situation of α-tocopherol/DPPC and α-tocopherol/DPPE systems at 280 K, while it moves much faster than lipid bilayers at the liquid-crystal phase, like the cases of all the systems at 350 K. At 310 K, it has a slower diffusion rate in DPPC than in the DPPE bilayer, which may be due to the fact that DPPE is more tightly packed than the DPPC bilayer and α-tocopherol tends to disturb the DPPE bilayer more drastically. This is in accordance with previous experimental reports that α-tocopherol induces the inverted hexagonal phase in the DPPE bilayer that coexisted with the lamellar gel phase of the pure phospholipid.[10] It has the fastest diffusion rate in the POPC bilayer at 310 K due to its highest fluidity. At 350 K, the diffusion rates of both α-tocopherol and phospholipids show an increasing sequential order of DPPE, DPPC, POPE, and POPC systems which is consistent with that of the corresponding pure lipids. Finally, we can see that the addition of α-tocopherol does not bring much change in the lateral diffusion rate of phospholipid molecules in all four lipid bilayers at all three examined temperatures.

3.5. Comparison with Cholesterol. It is worthwhile to compare the structural and kinetic properties of α-tocopherol and cholesterol. Both molecules consist of a hydrophobic tail and a ring-structured head with a hydroxyl group. The similar molecular structures suggest that they may behave similarly in plasma membranes. Comparing our results with previous simulation works on cholesterol/phospholipid systems, we do see both differences and similarities. Tu et al.[59] reported a 1.4 ns constant-pressure molecular dynamics simulation of cholesterol at 12.5 mol % in a DPPC bilayer at 50 °C and found that the cholesterol molecules prefer to have their hydroxyl oxygens below the DPPC phosphate groups. In our simulations, the preferred location of hydroxyl oxygens in α-tocopherol is below the ester groups. Later, Chiu et al.[60] applied a hybrid equilibration and sampling procedure for the atomic level simulation of a hydrated lipid bilayer to systems consisting of DPPC or POPC at low (~6%) cholesterol concentration. They made several

TABLE 3: Lateral Diffusion Coefficients of α-Tocopherol and Lipids at Various Temperatures ($\times 10^{-7}$ cm^2/s)

		α-tocopherol/DPPC	α-tocopherol/POPC	α-tocopherol/DPPE	α-tocopherol/POPE
280 K	α-tocopherol	1.9 ± 0.6	3.9 ± 0.4	1.9 ± 0.2	3.3 ± 0.7
	lipid	1.6 ± 0.3	3.7 ± 0.3	2.0 ± 0.2	3.5 ± 0.3
	pure lipid	1.2 ± 0.2	4.4 ± 0.5	1.6 ± 0.6	3.2 ± 0.9
310 K	α-tocopherol	2.8 ± 0.4	8.6 ± 0.6	4.5 ± 0.8	7.4 ± 0.8
	lipid	2.2 ± 0.5	6.8 ± 0.3	3.6 ± 0.6	5.8 ± 1.0
	pure lipid	3.6 ± 0.6	6.9 ± 0.6	3.4 ± 0.8	13.0 ± 1.5
350 K	α-tocopherol	16.8 ± 6.5	22.1 ± 4.1	10.9 ± 1.5	20.4 ± 0.8
	lipid	8.1 ± 1.1	12.4 ± 1.0	4.8 ± 0.5	11.3 ± 1.25
	pure lipid	8.7 ± 0.4	14.0 ± 0.3	7.6 ± 1.6	17.6 ± 1.4

conclusions: first, cholesterol could form hydrogen bonds with carbonyl oxygen in DPPC and POPC molecules; second, cholesterol has a larger tilt angle in POPC than in the DPPC bilayer due to the higher fluidity of the POPC bilayer; third, cholesterol diffuses slower than both DPPC and POPC lipid bilayers. We have similar results with their first and second conclusions. However, in our studies, the α-tocopherol molecule moves much faster than lipid molecules at high temperatures, which is in accordance with various experimental results reported before.[21] The difference in the dynamic feature of α-tocopherol and cholesterol molecules may be due to their different structures: α-tocopherol has a smaller head which attenuates the diffusion resistance and a longer tail which disturbs lipid bilayers. Considering the flip-flop behavior, Marrink et al.[61] used the MARTINI coarse-grained (CG) model to simulate the behavior of cholesterol inside the lipid bilayer at 300 K and observed a total number of 55 flip-flop events during the 60 μs simulation, with individual flip-flop times ranging from 100 ns to 15 μs. Our simulation for the α-tocopherol/POPC system shows that α-tocopherol would not flip-flop at 280 and 310 K and flips over at 350 K, which is consistent with previous experimental results that α-tocopherol is harder to flip-flop than cholesterol.[62] Because α-tocopherol has a more polar head than cholesterol and probably interacts with the lipid interface more favorably, α-tocopherol is more difficult to flip over than cholesterol.

4. Conclusions and Remarks

We simulated the systems of α-tocopherol with several model membranes at different temperatures to study the position, conformation, and dynamic properties of α-tocopherol in a few selected phospholipid bilayers. As we have discussed above, in all the four systems, it stays in one leaflet of lipid bilayers at 280 and 310 K and flips over from one side to the other at 350 K, and α-tocopherol flips faster in POPC and POPE than in DPPC and DPPE bilayers. This can be explained as a result of the higher fluidity of the former two phospholipids due to the presence of an unsaturated bond in the *sn*-2 acyl chain of the lipid molecules.

We also analyzed the average position of α-tocopherol's hydroxyl group relative to lipid tails. At 280 and 310 K, the hydroxyl oxygen locates at a position between C3′ and C5′ of the *sn*-2 acyl chain. With increasing temperature, the hydroxyl group moves toward the bilayer center. This would trigger the occurrence of the flip-flop of α-tocopherol molecules. Such temperature effect is considered as an entropic effect.

Hydrogen bond analysis shows that the hydrogen bonds are mainly with the glycerol−fatty acid ester groups, not with the phosphate group in a lipid molecule at all three temperatures. The hydrogen bonds involving phosphatidylethanolamines are more stable than that involving phosphatidylcholines at low temperatures, and the hydrogen bonds between the hydroxyl group of α-tocopherol and the amino group in the phosphatidylethanolamines can be ignored.

We also calculated tilt angle distribution curves of α-tocopherol head and tail groups. The results show that the head of α-tocopherol does not stay strictly vertical to the surface in lipid bilayers, and it has changing tilt angles with the maximum probability ranging from 10 to 37° when flip-flop does not occur. While α-tocopherol flips between the upper and lower leaflets, its headgroup has a broad distribution with two peaks corresponding to situations when α-tocopherol is in the two leaflets, and the α-tocopherol head tends to have a larger tilt angle when the lipid matrix is more fluid. Compared with the headgroup, the α-tocopherol acyl tail always has broader distributions corresponding to the more freely moving modes.

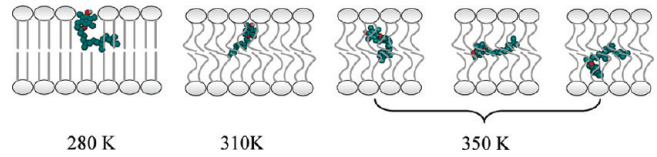

Figure 6. Model to depict the location and orientation of an α-tocopherol molecule in lipid bilayers at three temperatures.

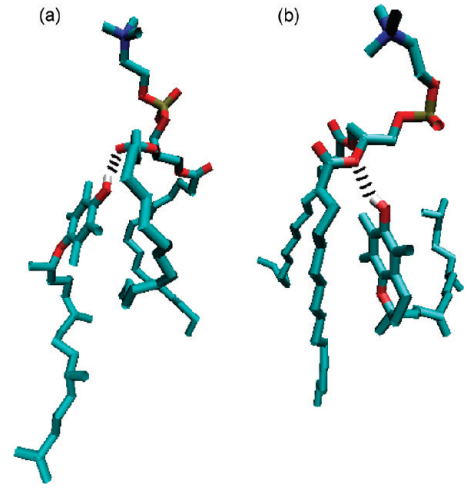

Figure 7. Snapshots showing α-tocopherol forming hydrogen bonds with different oxygen atoms in the DPPC headgroup: (a) carbonyl oxygen and (b) glycerol oxygen. Other nearby molecules have been omitted to emphasize the relevant details. Black dashed lines indicate hydrogen bonds.

The temperature-dependent features of the location and orientation of an α-tocopherol molecule in a phospholipid bilayer as discussed above are summarized in Figure 6. It should be noted that the alignments of α-tocopherol molecules are selected from representative snapshots, while the phospholipid molecules are just a schematic drawing. Details of the relative orientations of an α-tocopherol and a phospholipid molecule are further shown in Figure 7. This highlights the hydrogen bonds formed between the hydroxyl group of α-tocopherol and the ester group in the phospholipid molecule and the flexible orientation of the chains of both molecules.

The kinetic property of α-tocopherol in model membranes is also analyzed. We calculated the lateral diffusion coefficients of α-tocopherol and phospholipid molecules in bilayers. The results reveal that α-tocopherol has a comparable diffusion rate with the phospholipid molecules at low temperature, while it moves much faster than the lipids at high temperatures.

Acknowledgment. This work was supported by a grant from the Natural Science Foundation of China (20633080) and a "973" National Key Basic Research Program of China (2006CB806200). We are grateful to Prof. Peter J. Quinn for his insightful comments.

Supporting Information Available: Force field deduction process, force field for α-tocopherol, deuterium order parameter, and coordinates of atom O7 at 350 K. This material is available free of charge via the Internet at http://pubs.acs.org.

References and Notes

(1) Evans, H. M.; Bishop, K. S. *Science* **1922**, *56*, 650.
(2) Fernholz, E. J. *J. Am. Chem. Soc.* **1938**, *60*, 700.

(3) Sheppard, A. J.; Pennington, J. A. T.; Weihrauch, J. L. Analysis and distribution of vitamin E in vegetable oils and foods. In *Vitamin E in Health and Disease*; Packer, L., Fuchs, J., Eds.; Marcel Dekker: New York, 1993; p 9.

(4) Traber, M. G. *Free Radical Biol. Med.* **1994**, *2*, 229.

(5) Traber, M. G.; Ramakrishnan, R.; Kayden, J. H. *Proc. Natl. Acad. Sci. U.S.A.* **1994**, *91*, 10005.

(6) Kagan, V. E.; Annal, N. Y. *Acad. Sci.* **1989**, *570*, 121.

(7) Atkinson, J.; Epand, R. F.; Epand, R. M. *Free Radical Biol. Med.* **2008**, *44*, 739.

(8) Quinn, P. J. *Eur. J. Biochem.* **1995**, *233*, 916.

(9) Wang, X. Y.; Semmler, K.; Richter, W.; Quinn, P. J. *Arch. Biochem. Biophys.* **2000**, *377*, 304.

(10) Wang, X. Y.; Quinn, P. J. *Eur. J. Biochem.* **1999**, *264*, 1.

(11) Suzuki, Y.; Tsuchiya, M.; Wassall, S. R.; Govil, G.; Kagan, V. E.; Packer, L. *Biochemistry* **1993**, *32*, 10692.

(12) Wassall, S. R.; Thewalt, J. L.; Wong, L.; Gorrisen, H.; Cushley, R. J. *Biochemistry* **1986**, *25*, 319.

(13) Ohyashiki, T.; Ushiro, H.; Mohri, T. *Biochim. Biophys. Acta* **1986**, *858*, 294.

(14) Bisby, R. H.; Birch, D. J. S. *Biochem. Biophys. Res. Commun.* **1989**, *158*, 386.

(15) Shamovski, I. L.; Yrovskaya, I. Y. *J. Chim. Phys. Phys. - Chim. Biol.* **1991**, *88*, 2675.

(16) Srivastava, S.; Phadke, R. S.; Govil, G.; Rao, C. N. R. *Biochim. Biophys. Acta* **1983**, *734*, 353.

(17) Fragata, Y. M.; Bellemare, Y. F. *Chem. Phys. Lipids* **1980**, *27*, 93.

(18) Stillwell, W.; Ehringer, W.; Wassall, S. R. *Biochim. Biophys. Acta* **1992**, *1105*, 237.

(19) Kagan, V. E.; Quinn, P. J. *Eur. J. Biochem.* **1988**, *171*, 661.

(20) Takahashi, M.; Tsuchiya, J.; Niki, E. *J. Am. Chem. Soc.* **1989**, *111*, 6350.

(21) Gramlich, G.; Zhang, J. Y.; Nau, W. M. *J. Am. Chem. Soc.* **2004**, *126*, 5482.

(22) Buttriss, J. L.; Diplock, A. T. *Biochim. Biophys. Acta* **1988**, *963*, 61.

(23) Zhang, Y.; Turunen, M.; Appelkvist, E. L. *J. Nutr.* **1996**, *126*, 2089.

(24) Darden, T.; York, D.; Pedersen, L. *J. Chem. Phys.* **1993**, *98*, 10089.

(25) Essmann, U.; Perera, L.; Berkowitz, M. L.; Darden, T.; Lee, H.; Pedersen, L. G. *J. Chem. Phys.* **1995**, *103*, 8577.

(26) Berendsen, H. J. C. Transport properties computed by linear response through weak coupling to a bath. In *Computer Simulations in Material Science*; Meyer, M., Pontikis, V., Eds.; Kluwer: Dordrecht: The Netherlands, 1991.

(27) Berendsen, H. J. C.; Postma, J. P. M.; DiNola, A.; Haak, J. R. *J. Chem. Phys.* **1984**, *81*, 3684.

(28) Berendsen, H. J. C.; van der Spoel, D.; van Drunen, R. *Comput. Phys. Commun.* **1995**, *91*, 43.

(29) Lindahl, E.; Hess, B.; van der Spoel, D. *J. Mol. Model.* **2001**, *7*, 306.

(30) http://www.ucalgary.ca/tieleman/download.html.

(31) Ryckaert, J. P.; Bellemans, A. *Chem. Phys. Lett.* **1975**, *30*, 123.

(32) Berger, O.; Edholm, O.; Jähnig, F. *Biophys. J.* **1997**, *72*, 2002.

(33) Jorgensen, W. L.; Tirado-Rives, J. *J. Am. Chem. Soc.* **1988**, *110*, 1657.

(34) Essex, J. W.; Hann, M. M.; Richards, W. G. *Philos. Trans. R. Soc. B* **1994**, *344*, 239.

(35) Chiu, S. W.; Clark, M.; Balaji, V.; Subramaniam, S.; Scott, H. L.; Jakobsson, E. *Biophys. J.* **1995**, *69*, 1230.

(36) Berendsen, H. J. C.; Postma, J. P. M.; van Gunsteren, W. F.; Hermans, J. *Intermolecular Forces*; Reidel, Dordrecht: The Netherlands, 1981.

(37) Miyamoto, S.; Kollman, P. A. *J. Comput. Chem.* **1992**, *13*, 952.

(38) Yang, L. J.; Tan, C. H,; Hsieh, M. J.; Wang, J. M.; Duan, Y.; Cieplak, P.; Caldwell, J.; Kollman, P. A.; Luo, R. *J. Phys. Chem. B* **2006**, *110*, 13166.

(39) Pearlman, D. A.; Case, D. A.; Cadwell, J. W.; Ross, W. S.; Cheatham, T. E., III; DeBolt, S.; Ferguson, D.; Siebel, G.; Kollman, P. *Comput. Phys. Commun.* **1995**, *91*, 1.

(40) Frisch, M. J.; Trucks, G. W.; Schlegel, H. B.; Scuseria, G. E.; Robb, M. A.; Cheeseman, J. R.; Zakrzewski, V. G., Montgomery, J. A., Jr.; Stratmann, R. E., Burant, J. C., Dapprich, S.; Millam, J. M.; Daniels, A. D.; Kudin, K. N.; Strain, M. C.; Farkas, O.; Tomasi, J.; Barone, V.; Cossi, M.; Cammi, R.; Mennucci, B.; Pomelli, C.; Adamo, C.; Clifford, S.; Ochterski, J.; Petersson, G. A.; Ayala, P. Y.; Cui, Q.; Morokuma, K.; Malick, D. K., Rabuck, A. D.; Raghavachari, K.; Foresman, J. B.; Cioslowski, J.; Ortiz, J. V.; Stefanov, B. B.; Liu, G.; Liashenko, A.; Piskorz, P.; Komaromi, I.; Gomperts, R.; Martin, R. L.; Fox, D. J.; Keith, T.; Al-Laham, M. A.; Peng, C. Y.; Nanayakkara, A.; Gonzalez, C.; Challacombe, M.; Gill, P. M. W.; Johnson; B.; Chen, W.; Wong, M. W.; Andres, J. L.; Gonzalez, C.; Head-Gordon, M.; Replogle, E. S.; Pople, J. A. *Gaussian 98*, Revision A.3; Gaussian, Inc.: Pittsburgh, PA, 1998.

(41) Bayly, C. I.; Cieplak, P.; Cornell, W. D.; Kollman, P. A. *J. Phys. Chem. B* **1993**, *97*, 10269.

(42) http://en.wikipedia.org/wiki/Tocopherol.

(43) Min, K. C.; Kovall, R. A.; Hendrickson, W. A. *Proc. Natl. Acad. Sci. U.S.A.* **2003**, *100*, 14713.

(44) Jorgensen, W. L.; Maxwell, D. S.; Tirado-Rives, J. *J. Am. Chem. Soc.* **1996**, *118*, 11225.

(45) Jorgensen, W. L.; McDonald, N. A. *THEOCHEM* **1998**, *424*, 145.

(46) Jorgensen, W. L.; McDonald, N. A. *J. Phys. Chem. B* **1998**, *102*, 8049.

(47) Rizzo, R. C.; Jorgensen, W. L. *J. Am. Chem. Soc.* **1999**, *121*, 4827.

(48) Watkins, E. K.; Jorgensen, W. L. *J. Phys. Chem. A* **2001**, *105*, 4118.

(49) Kaminski, G. A.; Friesner, R. A.; Tirado-Rives, J.; Jorgensen, W. L. *J. Phys. Chem. B* **2001**, *105*, 6474.

(50) Leekumjorn, S.; Sum, A. K. *Biochim. Biophys. Acta* **2007**, *1768*, 354.

(51) Luzar, A.; Chandler, D. *J. Chem. Phys.* **1993**, *98*, 8160.

(52) Luzar, A.; Chandler, D. *Nature* **1996**, *397*, 55.

(53) Lefevre, T.; Picquart, M. *Biospectroscopy* **1996**, *2*, 391.

(54) Pink, D. A.; McNeil, S.; Quinn, B.; Zuckermann, M. J. *Biochim. Biophys. Acta* **1998**, *1368*, 289.

(55) Leekumjorn, S.; Sum, A. K. *J. Phys. Chem. B* **2007**, *111*, 6026.

(56) Fahey, P. F.; Koppel, D. E.; Barak, L. S.; Wolf, D. E.; Elson, E. L.; Webb, W. W. *Science* **1977**, *195*, 305.

(57) Filippov, A.; Oradd, G.; Lindblom, G. *Biophys. J.* **2003**, *84*, 3079.

(58) Klauda, J. B.; Venable, R. M.; MacKerell. A. D., Jr.; Pastor, R. W. Considerations for Lipid Force Field Development. In *Computational Modeling of Membrane Bilayers*; Feller, S. E., Ed.; Elsevier.

(59) Tu, K.; Klein, M. L.; Tobias, D. J. *Biophys. J.* **1998**, *75*, 2147.

(60) Chiu, S. W.; Jakobsson, E.; Scott, H. L. *Biophys. J.* **2001**, *80*, 1104.

(61) Marrink, S. J.; de Vries, A. H.; Harroun, T. A.; Katsaras, J.; Wassall, S. R. *J. Am. Chem. Soc.* **2008**, *130*, 10.

(62) Tyurin, V. A.; Kagan, V. E.; Serbinova, E. A.; Gorbunov, N. V.; Erin, A. N.; Prilipko, L. L.; Stoichev, Ts. S. *Bull. Exp. Biol. Med.* **1986**, *102*, 1677.

JP9074306